Effectiveness of staff radiation protection devices for interventional cardiology procedures

Christelle Huet, Jérémie Dabin, Joanna Domienik-Andrzejewska, Alexandre Hebre, Edilaine Honorio da Silva, Pasquale Lombardo, Giulia Tamborino, Filip Vanhavere

Physica Medica 107 (2023) 102543

Contents lists available at ScienceDirect

Physica Medica

journal homepage: www.elsevier.com/locate/ejmp

Effectiveness of staff radiation protection devices for interventional cardiology procedures

Christelle Huet [a,*], Jérémie Dabin [b], Joanna Domienik-Andrzejewska [c], Alexandre Hebre [a], Edilaine Honorio da Silva [b], Pasquale Lombardo [b], Giulia Tamborino [b], Filip Vanhavere [b]

[a] Institut de radioprotection et de sûreté nucléaire, Pôle santé et environnement, Service de recherche en dosimétrie, Fontenay-aux-Roses, France
[b] Belgian Nuclear Research Centre, Research in Dosimetric Applications, Mol, Belgium
[c] Nofer Institute of Occupational Medicine, Department of Radiation Protection, Łódź, Poland

ARTICLE INFO

Keywords:
Interventional radiology
Radioprotective device
Effectiveness
Monte Carlo simulations

ABSTRACT

Purpose: To evaluate the effectiveness of currently available radioprotective (RP) devices in reducing the dose to interventional cardiology staff, especially to the eye lens and brain.
Methods: The performances of five RP devices (masks, caps, patient drapes, staff lead and lead-free aprons and Zero-Gravity (ZG) suspended radiation protection system) were assessed by means of Monte Carlo (MC) simulations. A geometry representative of an interventional cardiology setup was modelled and several configurations, including beam projections and staff distance from the source, were investigated. In addition, measurements on phantoms were performed for masks and drapes.
Results: An average dose reduction of 65% and 25% to the eyes and the brain respectively was obtained for the masks by MC simulations but a strong influence of the design was observed. The cap effectiveness for the brain ranges on average between 13% and 37%. Nevertheless, it was shown that only some upper parts of the brain were protected. There was no significant difference between the effectiveness of lead and lead-free aprons. Of all the devices, the ZG system offered the highest protection to the brain and eye lens and a protection level comparable to the apron for the organs normally covered.
Conclusion: All investigated devices showed potential for dose reduction to specific organs. However, for masks, caps and drapes, it strongly depends on the design, exposure conditions and staff position. Therefore, for a clinical use, it is recommended to evaluate their effectiveness in the planned conditions of use.

Introduction

Fluoroscopically-guided interventional procedures associate a radiological imaging technique (using low energy X-rays) and a minimally invasive procedure with diagnostic or therapeutic aim. Using imaging enables to guide the surgeon and to do less invasive surgeries. Thus, interventional procedures in cardiology are techniques that have had widely spread in the last decades. Although interventional cardiology (IC) enables less invasive surgeries, there are concerns about the exposure of both the patient and the staff. Regarding medical staff working in IC, they are mainly exposed to scattered ionizing radiation.

The interventional staff receives the highest eye lens doses of ionising radiations in the medical sector, with cumulative eye lens doses ranging from a few mSv up to a few Sv over their entire career [1]. Since the early 2010s, several studies have reported an elevated incidence of eye lens opacities typically associated with ionising radiations among the interventional staff especially in cardiology [2–4].

Recently, studies have reported the occurrence of brain tumours among interventional radiologists and cardiologists [5–7] and a prospective cohort assessment indicated a twofold increased risk for brain cancer mortality compared to unexposed controls [8]. In particular, in the study of Roguin *et al.* [6], a disproportionate incidence of left-sided brain tumours (85 %) was observed. Given that the left side of the interventional cardiologist head is known to be more exposed to radiation than the right one, these findings raise concern.

Thus, there has been an increasing interest in radiation protection devices that offer shielding in particular to the head. Many devices are available to protect the staff: from frequently used equipment, such as lead glasses or ceiling-suspended screen, to drapes positioned on the patient or the ceiling- suspended cabins (e.g. Zero-Gravity (ZG) system).

* Corresponding author.
E-mail address: christelle.huet@irsn.fr (C. Huet).

https://doi.org/10.1016/j.ejmp.2023.102543
Received 20 April 2022; Received in revised form 13 January 2023; Accepted 3 February 2023
Available online 11 February 2023

However, estimating the actual dose reduction effectiveness of those devices remains challenging because it can be strongly affected by their design and by the exposure conditions. Among other activities, the MEDIRAD project (Implications of medical low dose radiation exposure) aims to bridge gaps in the knowledge of staff radiation protection. In this framework, the effectiveness of currently available radioprotective (RP) devices in reducing the dose to interventional cardiology staff, especially to the eye lens and brain, was investigated. From an extensive literature review carried out at the beginning of the project, ten different RP devices were identified [9]. A need for additional investigations was identified for five of them: masks, caps, patient drapes, staff lead and lead-free aprons and the Zero-Gravity suspended radiation protection system. As a matter of fact, for some of the RP devices, a limited number of publications was available: for the mask, only one publication presenting attenuation measurements in laboratory conditions [10] and for the lead-free apron no publication about effectiveness in clinical settings whether measured or simulated with MC. For others (drape and ZG system), the effectiveness was only investigated by means of clinical measurements [11–13] which is not sufficient to assess the dose savings to the brain [14] and, in a lesser extent, to the eyes. For the cap, clinical studies investigated the dose savings to the brain with the same limitations [15–16]; two studies included MC simulations in addition to measurements; however, the number of configurations evaluated was rather limited [14,17].

In the framework of the MEDIRAD project, the performances of the five devices were assessed by means of Monte Carlo (MC) simulations and measurements on staff and phantoms. This article presents the results of the MC simulations for the five devices and of phantom measurements for two devices (mask and drape); results of the measurement campaigns on staff are presented elsewhere [9,11–13]. The purpose of the present study was: (1) to assess the dose reduction effectiveness of RP tools, especially for the eye lens and the brain, (2) to identify the parameters influencing the dose reduction effectiveness (irradiation parameters as well as RP tool intrinsic parameters) and (3) to compare the"real" dose reduction effectiveness of the RP device (assessed at the level of the organs) to the one commonly estimated from measurements on staff.

Material and methods

Monte Carlo simulations were performed for the five RP devices to calculate their potential for reducing exposure of various organs at the settings commonly used during IC procedures. In addition, the correlation between the "real" effectiveness (calculated at the level of the organs) and the effectiveness as commonly estimated from measurements on staff (calculated at the level of the dosimeters) was investigated.

Interventional cardiology setup

A geometry representative of an interventional cardiology setup was simulated using MCNPX [18] and MCNP 6.2 [19] MC codes. The examination settings and their values are listed in Table 1. Five X-ray beam projections, commonly used in clinical practice during IC procedures, were considered, namely postero-anterior (PA), left anterior oblique at 45° and 90° (LAO45 and LLAT) and right anterior oblique at 45° and 90° (RAO45 and RLAT). Two standing positions of the operator were considered: 40 cm and 70 cm from the centre of X-ray field on the right side of the patient, representing radial and femoral access, respectively. For the ZG device, only the position at 70 cm was simulated since it was not possible to model the position at 40 cm due to its bulkiness. Finally, two orientations of the operator's head were modelled: forward and 30° away from the X-ray tube.

Table 1
Examination settings and values used for the simulations.

Examination settings	Values
Use of RP device	With - without
Beam projections	PA, LAO45, LAO90, RAO45, RAO90
Operator's distance from the X-ray field	40 and 70 cm
Operator's head orientation	forward (0°) and 30° away from the X-ray tube
Field size at the detector (cm)	30 × 30: PA, LAO45 and RAO45 20 × 20: LLAT and RLAT
X-ray energy spectrum	80 kV, 3 mm Al
Source-to-patient-skin entrance distance (cm)	60
Source-to-image-detector distance (cm)	90
Patient-to-image-detector distance (cm)	10

An X-ray spectrum corresponding to a tube voltage of 80 kV with a filtration of 3 mm Al was used. The X-ray photons were emitted from a point source into a cone and collimated into a square field of 20 × 20 cm^2 or a 30 × 30 cm^2, depending on the projection, at the entrance of the image detector. The source-to-image-detector distance was fixed (90 cm); the source-to-patient skin entrance distance and the patient-to-image-detector distance was set to 60 cm and 10 cm in PA, respectively, and could change, due to beam rotation, for the remaining projections. The image detector was modelled by a hollow lead box (2 mm Pb on the side, 5 mm Pb on top and containing air inside) with a 1.5 mm thick Al window on the entrance side above the patient. No RP room equipment was modelled since we wanted to investigate the effectiveness of the devices separately.

Numerical phantoms

Three kinds of numerical phantoms are available for MC simulations: stylized, voxel and hybrid phantoms. In stylized phantoms the organs are defined from a combination of mathematical equations which describe elliptical surfaces, cylindrical surfaces, etc. The advantages of these phantoms are smooth surfaces and flexibility – they can be modified by appropriate changes in parameters of the equations they are described with. However, the anatomical realism is limited, especially regarding the shape and the location of the organs. Voxel phantoms are created from CT or MRI of patients or corpses. Thus, these phantoms are representative of the anatomy, but they are hardly flexible and so can hardly be modified in terms of posture and morphology. Finally, hybrid phantoms are based upon non-uniform rational B-spline (NURBS) and/or polygon mesh surfaces. They combine the advantages of both stylized and voxel phantoms, namely flexibility and anatomical realism.

All in all, five different numerical phantoms were constructed from the three kinds of phantoms described above and used in the simulations: one for the patient and four for the interventional cardiologist, selected on a case-by-case basis according to the type of protection being studied. A single simple stylized phantom was used for the patient [20]. There is no distinction between the different organs, only a simplified skeleton and the lungs are modelled in the patient. Regarding the cardiologist, one phantom was used for the study of masks and caps, a second for the study RP drapes; a third for the study of aprons; and a fourth for the study of the ZG device. These phantoms are detailed in Table 2. For the study of masks and caps, the phantom constructed by Silva *et al.* [14] was used. In addition, for this study, the voxelised head has been specially modified to include the detailed ICRP eye lens model, which considers the sensitive and insensitive volumes of the eye lens separately [25] (Fig. 1). Regarding ZG device, a voxelised phantom was created from the realistic anthropomorphic flexible polygonal mesh phantom developed by Lombardo *et al.* [28–29].

Modelling of the radioprotective devices

Masks

Several masks are commercially available. Two of them (VIS400 face mask (Longkou Sanyi Medical Device Co., China) and Full face style mask (Philips Safety products, USA)) were chosen (Fig. 2) (named M1 and M2). They are both composed of an acrylic and lead mixture whose

Table 2
Numerical phantoms used for the operator modelling for the five radioprotective devices investigated.

RP device	Organs of interest	Phantom
Mask	Brain tissue; Eye lens	Mathematical phantom [21–23] + voxelised head [24] + detailed eye lens model [21] as per [14]
Lead-free and leaded caps	Brain tissue	Same as for the mask
RP drapes	All organs not covered by the apron Brain tissue; Eye lens	Mathematical phantom [20–21] with hands on the patient Same as for the mask
Lead-free and light-lead aprons	All organs under the apron	ICRP male phantom [26] equipped with an apron [27]
Zero-Gravity system	All organs	Voxelised flexible phantom [28–29]

exact proportions are unknown. As such, they were modelled using the lead equivalence of 0.1 mm announced by the manufacturer. However, their shapes are quite different which could influence their protective capabilities for organs located in the head. Thus, a third mask (named M1L), not available, was also modelled as M1 with a 7.8 cm longer screen, so that it had the same length as M2 in order to study the effect of the length.

For M1 and M2, four pairs of dosimeters were placed above and below the mask at four different positions (left lower and higher rim and right lower and higher rim) in order to evaluate its effectiveness as commonly estimated from measurements on staff. Dosimeters were modelled by cylinders (0.16 cm^3) made of soft tissue material. Finally, an eye lens ($H_p(3)$) dosimeter was modelled on the left temple of the numerical phantom (Fig. 2).

Caps

The shape of the commercially available caps is quite similar from one model to another. In order to study the effect of the cap composition on its effectiveness, one cap model with two different compositions (pure lead and a lead-free metal alloy) was modelled. The cap model is based on a commercial surgical model (RADPAD No Brainer X-ray Protective Surgical Cap; Worldwide Innovations & Technologies) which is 12 cm high and covers the head obliquely from above the eyebrows and the nape (Fig. 3). The top of the head is unshielded.

Dose reduction of caps has been reported in the literature by staff measurements using dosimeters placed above and below [16,30]. Three pairs of dosimeters made of soft tissue material were simulated above and below the cap. They were placed near the left temple, at the forehead between the eyes and at the end of the left eyebrow (Fig. 3). Finally, an eye lens ($H_p(3)$) dosimeter was modelled directly on the left temple of the numerical phantom.

Patient drapes

A commercially available lead-free drape (0.375 mm Pb eq) was modelled. The material composition was obtained from the manufacturer under a non-disclosure agreement. Although the manufacturer advised different drape positions depending on the access route (represented in the MC simulations by the interventional cardiologist position with respect to the X-ray beam centre), this could not be implemented. Positioning the drape closer to the patient chest as advised for a radial or brachial access route would have resulted in the drape interacting with the primary beam. Only one drape position was therefore considered for the simulation set-ups (Fig. 4). An eye lens ($H_p(3)$) dosimeter was modelled on the left temple and a whole-body (WB, $H_p(10)$) dosimeter on the left side of the chest above the apron, in order to evaluate the drape effectiveness as derived from measurements on staff in clinical studies. In addition, to assess the effect on the skin extremities, thin tallying regions (1-mm thickness) were defined at the palm and forearm surface facing the patient.

Staff lead and non-lead aprons

Three full-body apron models with different compositions were studied. Pure lead (LA) and two lead-free compositions, based on manufacturer data (LFA1) and on data from experimental characterization (LFA2) [31], were modelled (Table 3). All aprons had the same design, only the effect of the material composition and/or the actual thickness were considered. For each apron, a thyroid collar with the same thickness and composition was also modelled. Finally, a pair of dosimeters was placed on the left side of the chest above and below the apron.

Zero-Gravity suspended radiation protection system

The ZG (Biotronik, Germany) was modelled based on the information provided by the manufacturer: an apron with lead thickness varying between 0.5 and 1 mm for the apron and the arm flaps, depending on the location, and 0.5 mm for the face shield. The model was then included in a software enabling fast generation of MCNP input files (Fig. 5) [29]. As

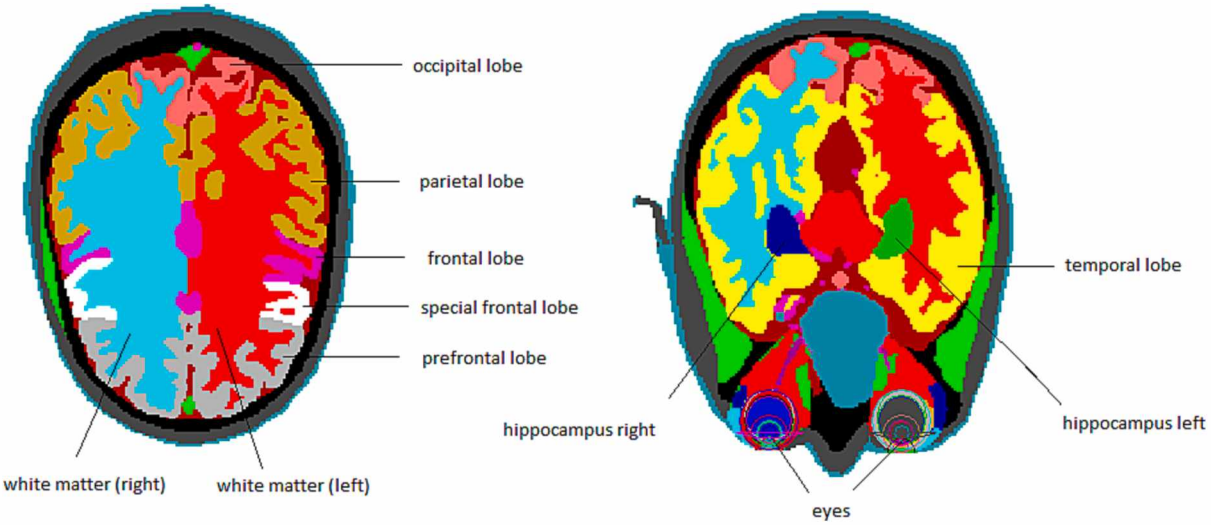

Fig. 1. Voxelised head phantom including detailed brain and eye lens structures.

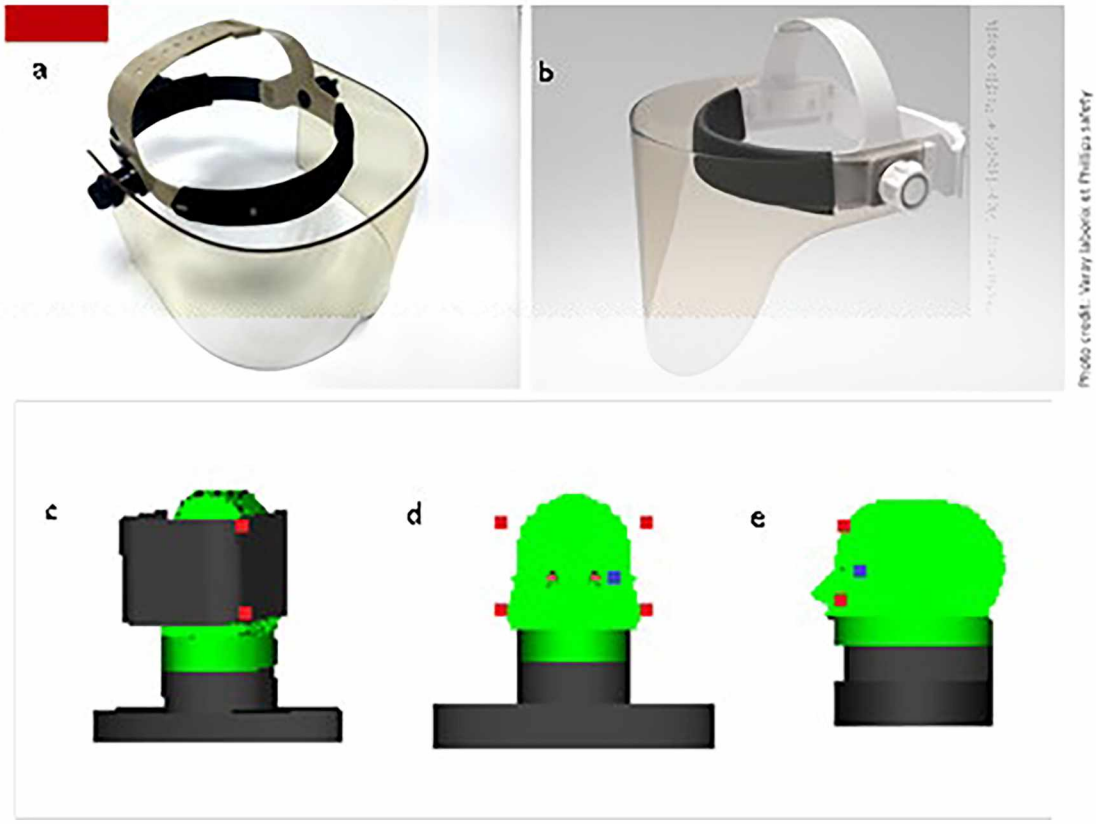

Fig. 2. Pictures of the commercial masks modelled in the MC simulations a: M1, b: M2, c: frontal view of the cardiologist model with the M1 mask, d frontal and e: lateral view of the cardiologist model without the mask; dosimeters are represented in red (soft tissue dosimeters positioned above and under the mask) and blue (eye lens). Dosimeters were enlarged for visualisation purpose.

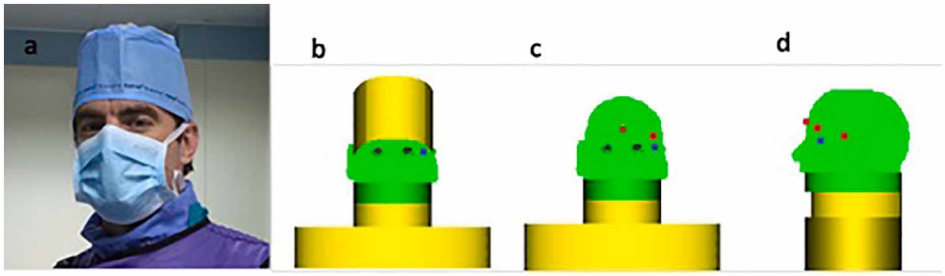

Fig. 3. a: Picture of the cap modelled (RADPAD No Brainer X-ray Protective Surgical Cap; Worldwide Innovations & Technologies; source: http://www.varaylaborix.com), b: frontal view of the cardiologist model with the cap, c: frontal and d: lateral view of the cardiologist model without the cap; dosimeters are represented in red (soft tissue) and blue (eye lens). Dosimeters were enlarged for visualisation purpose.

already mentioned, due to its bulkiness it was not possible to simulate the operator at 40 cm from the source. A WB ($H_p(10)$) dosimeter was added on the left side of the cardiologist chest, above the apron when used, and below the ZG otherwise.

Monte Carlo simulations settings and data analysis

The default MCNP physical parameters for photon transport (i.e. including fluorescence and energy cut-off set to 1 keV) and ENDF/B-VI libraries were used. The DXTRAN variance reduction method was used [18]. This method enables to increase the number of particles in the region of interest. In this study, the DXTRAN sphere was placed around the operator's head.

The energy deposition, in MeV/g, in different organs or tissues and dosimeters was calculated by using MCNPX/MCNP F6:p tally. This tally uses the kerma approximation (energy from electrons created by photon interactions is assumed to be deposited locally). Some simulations were performed with and without this approximation (tally *F8) in order to verify that it was valid in our case (thin volumes for dosimeters).

For the drape, the apron and the ZG system, the effective dose was calculated applying ICRP 103 [32] formalism on the organ and tissue doses. The effective dose was not considered for the cap and the mask as with these RP devices only the head region might be protected.

The dose reduction effectiveness (expressed in %), also called effectiveness in the paper, of the RP device for the different organs investigated and for a given projection was calculated as the difference between the absorbed dose without the device (the control dose, D_C) and the dose with the RP device (D_{RP}), normalized to the dose without the device:

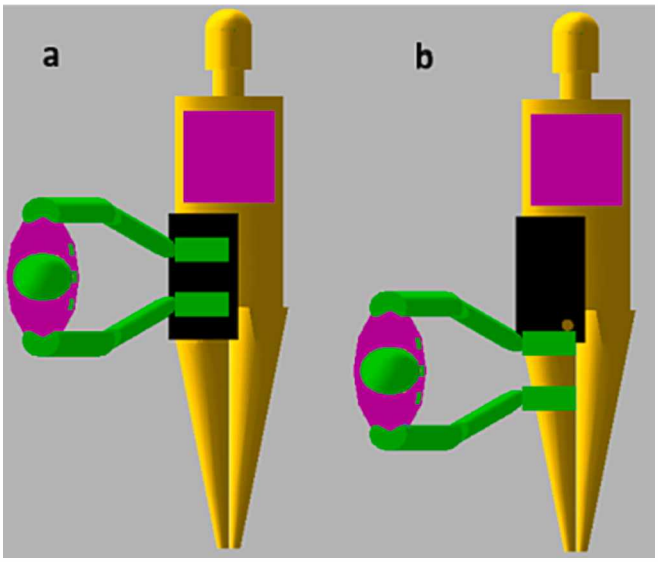

Fig. 4. Top view from the ORNL-ORAMED phantoms used for investigation of drape effectiveness. The cardiologist is positioned at a: 40 cm and b: 70 cm from the X-ray beam centre. The radioprotective drape is coloured in black; the image detector in purple.

Table 3
Characteristics of the lead and lead-free aprons investigated.

Apron	Composition	Density	Thickness (mm)
Lead apron (LA)	Pb	11.35	0.5
Lead-free apron 1 (LFA1)	Sb + Bi	4.8	0.5
Lead-free apron 2 (LFA2)	Sb + Bi	3.3	1.2

$$\frac{D_C - D_{RP}}{D_C} \quad (1)$$

Attenuation (expressed in %) was calculated for dosimeters placed above and under the caps and the masks as the difference between the dose absorbed above (D_A) and below the RP device (D_B), normalized to the dose above the device:

$$\frac{D_A - D_B}{D_A} \quad (2)$$

Phantom measurements

In order to further validate the results of the MC simulations, results were compared with measurements on anthropomorphic phantoms in clinical configurations. Results of such experiments being already available in the literature for the caps [33], the drapes (partially: [34]) and the ZG [13], complementary measurements were performed for the mask and the drape only.

A Rando Alderson (RA) phantom [35] and a PMMA phantom were set to represent the cardiologist and the patient, respectively. The RA phantom represents a 1.75 m tall and 73.5 kg male adult, without arms or legs, and is composed of multiple slices of tissue-equivalent material. The RA phantom was placed next to the operating table in the location corresponding to the position of cardiologist performing a real procedure. The head of the RA phantom was filled with 138 TLDs. This enabled the estimation of the dose to the brain (including cerebellum) and to the complete head region. For the evaluation of the exposure at the level of the left temple and both eye lens, three loose dosimeters were placed at each location during single exposure.

Measurements were performed on a C-arm Philips BV unit (Philips, The Netherlands). For each configuration, measurements were done sequentially with and without the RP device. Measurements were performed using three (PA, LAO 30 and LLAT) to four (PA, LAO 30, LLAT and RAO 30) beam projections for the drape and the mask respectively. Those beam projections were selected because of their significant frequency of use (PA, LAO 30 and RAO 30) and their potential for high staff exposure (LLAT). When the beam projection was changed, all other geometrical parameters were kept constant. Additional filtration and tube voltage of the X-ray unit were selected in the former case automatically while in the latter manually; the corresponding values were 3.0 mmAl and 90 kV. Although it was strived to achieve identical tube output levels (P_{KA}) for similar configurations, measurement results were normalised to the P_{KA}. Effectiveness of the RP device was calculated as per Equation (1).

A picture of the set-up is presented in Fig. 6. The distance of the RA phantom from the centre of the beam incident on the patient was 60 cm and the field size was 20 cm at the image detector position.

Results

For masks and caps simulations, statistical uncertainties were below 1 % for the brain, between 1 % and 3 % for eye lens and eye lens ($H_p(3)$) dosimeter and below 5 % for the other dosimeters. For the aprons, statistical uncertainty on effective dose was less than 1 %. For the drape

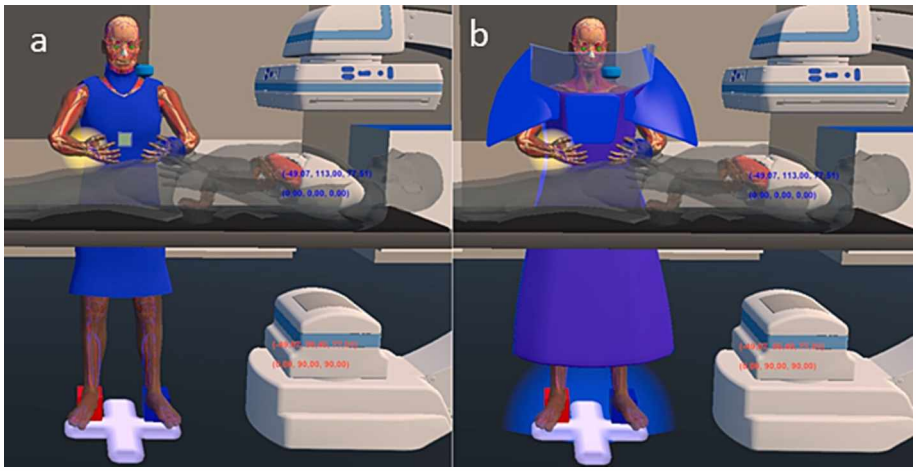

Fig. 5. Flexible numerical phantom equipped with a: apron and b: the ZG suspended system (screenshot from the software tool used for MCNP input file generation). The yellow halo on the right arm, the blue sphere on the left one and the green cylinder on the left shoulder and the cross on the ground are elements used for visualization and modification of the phantom posture. They are not modelled in the simulations.

Fig. 6. Measurement of the effectiveness of a mask (model M1) and a lead drape (LITE TECH, Inc., USA) on a RA phantom in a clinical set-up: a: position of dosimeters on the left temple and the eye lens, b: LAO 30 projection with neither mask nor drapes, c:LAO 30 projection with the mask d: LAO 30 projection with the lead drape.

simulations, uncertainties were below 1 % for the brain; below 3 % and 8 % for the eye lens and eye lens dosimeter, respectively; and below 4 % and 1 % for the WB dosimeter and the effective dose, respectively. For the ZG simulations, the uncertainties were less than 2 % for the brain; for the eye lens and the WB dosimeter, the uncertainties were below 1 % when the ZG was not used and up to 7 % and 12 % when the ZG was used, respectively; and below 1 % for the effective dose.

Masks

M1 and M2 masks attenuation obtained from the dosimeters placed at different locations above and below the mask averaged over the five simulated projections is given in Table 4. While attenuation for M1 is similar whatever the location of the dosimeters, a lower attenuation is observed for M2 for the dosimeters located on the right higher rim, in particular at 70 cm. However, the attenuation for a given distance is comparable between the two masks.

M1 mask effectiveness in reducing the doses to the sensitive volume of the eye lens, brain and $H_p(3)$ dosimeter obtained from MC calculations for the different projections and the two distances investigated (head at 0°) is presented in Fig. 7. The effectiveness from phantoms measurements at 60 cm is presented in Table 5. For all projections, a better simulated effectiveness is obtained at 70 cm compared to 40 cm. Additional simulations performed at 50 cm and 60 cm for PA projection indicate that the effectiveness in reducing the doses to $H_p(3)$ dosimeter increases from 3 % to 19 % between 50 cm and 60 cm and from 19 % to 59 % between 60 cm and 70 cm. Regarding the whole brain, it increases by step of 10 % between 40 cm and 70 cm, ranging from 11 % to 39 %.

Whatever the projection and the distance, M1 effectiveness in protecting the eye lens is poor. In the case of the right eye lens, the effectiveness obtained from phantom measurements is negative for LLAT and this is rather due to statistical reasons than the actual dose increase due to the presence of the mask. At 70 cm (Fig. 7), the effectiveness in reducing the doses to $H_p(3)$ dosimeter is around 65 % which is more than 8-fold the reduction for the sensitive volume of the eye lens, and at 60 cm (Table 5) it is on average 7-fold. Effectiveness for the brain averaged over the projections is around 12 % at 40 cm and 60 cm and 43 % at 70 cm.

M1, M1L and M2 simulated effectiveness for eye lens, brain and $H_p(3)$ dosimeter for the head at 0° and 30° and the two distances investigated is presented in Fig. 8. Effectiveness is averaged over the five projections. Regarding M1, no significant difference is observed between the head at 0° and the head at 30°, except for the shielding effectiveness to the brain which is enhanced by 15 % at 40 cm when the head is rotated. M1L, which is a lengthened version of M1, is much more efficient than M1 for the brain (62 %), the eye lens (64 % (left)) and $H_p(3)$ dosimeter (84 %) at 40°cm as well as at 70 cm, especially for the brain and the eye lens. Finally, with the head at 0°, M2 is very efficient for eye lens (70 % (left)) and $H_p(3)$ (60 %) and to a lesser extent for the brain (20 %) at 40 cm and 70 cm. Besides, it drops down to a few percent with the head rotated at 30° for both distances.

Caps

Simulated dose reduction effectiveness averaged over the five projections for a same operator distance and head position with the lead and lead-free caps is given in Table 6; little difference was observed between the projections (standard deviation always < 5 %, not shown). Results obtained for the two caps are very similar. The effectiveness for the brain is low, especially at 40 cm. It is improved when the head is rotated at 30°. However, whatever the head orientation, some parts of the brain are more protected than others (Fig. 9). As expected, both caps are ineffective to reduce the eye lens dose (less than 1 %).

Depending on the dosimeter location, the calculated cap attenuation differs considerably (Fig. 10). The attenuation obtained from the dosimeters located near the left eyebrow and on the left temple is quite similar (around 88 %) and does not vary much whatever the projection, the head position (0° or 30°) and the operator position (40 cm or 70 cm). By contrast, the attenuation obtained from the dosimeters located between the eyes is less than the one obtained from the two other dosimeter positions and varies considerably according to the projection, the head orientation and the operator location. A lower attenuation is obtained with LLAT projection for the head at 0° for both operator positions. Finally, with the head rotated at 30° the cap attenuation drops, especially for LAO and LLAT (values below 0) for both operator positions.

Table 4
M1 and M2 masks attenuation obtained from the dosimeters placed at different locations above and below the mask averaged over the five simulated projections at 40 cm and 70 cm.

	Mask M1				Mask M2			
	Left lower rim	Right lower rim	Left higher rim	Right higher rim	Left lower rim	Right lower rim	Left higher rim	Right higher rim
70 cm	76 %	80 %	82 %	76 %	81 %	77 %	84 %	65 %
40 cm	82 %	82 %	87 %	81 %	90 %	83 %	90 %	78 %

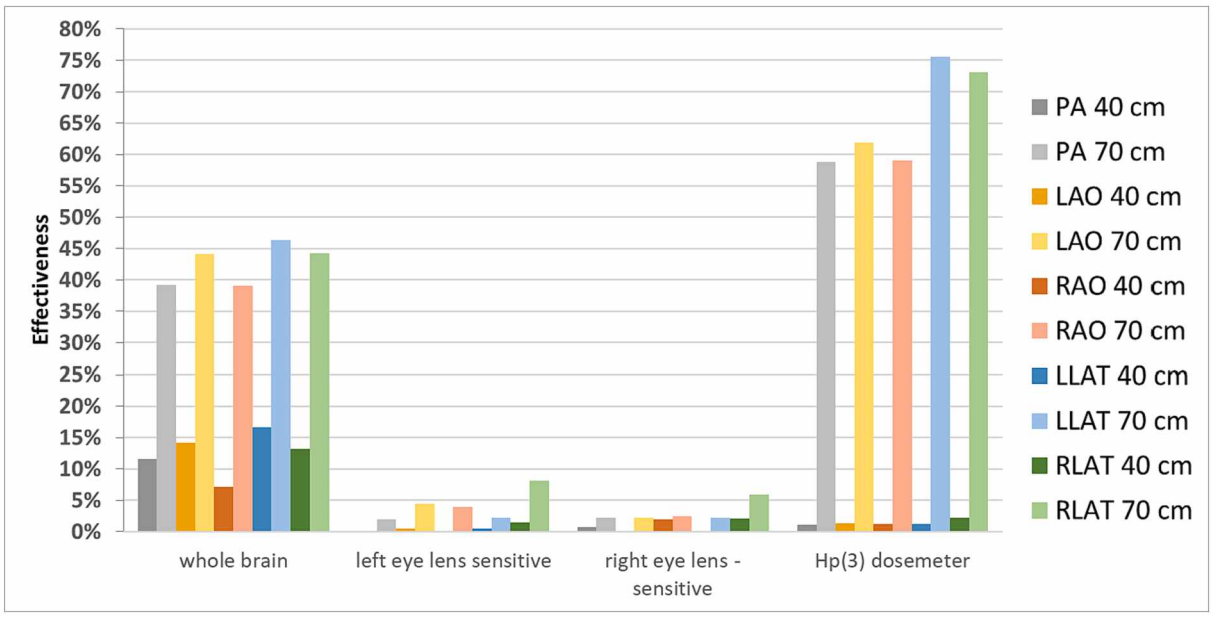

Fig. 7. M1 simulated dose reduction effectiveness for brain, eye lens and $H_p(3)$ dosimeter for the different projections and the two distances investigated (head at 0°). The brain includes the white matter and the lobes.

Table 5
M1 mask effectiveness resulting from phantom measurements. The phantoms distance from the X-ray field is 60 cm.

Anatomical region	PA	LAO 30	LLAT	RAO 30
Brain*	33 %	42 %	50 %	46 %
Brain including cerebellum	5 %	14 %	17 %	14 %
Head	12 %	15 %	20 %	16 %
Left temple	43 %	38 %	68 %	–
Left eye lens	10 %	10 %	0 %	–
Right eye lens	–	9 %	−2%	–

*Including frontal lobe and part of parietal lobe and the skull.

Aprons

Simulated dose reduction effectiveness obtained for the lead (LA) and the two lead-free aprons (LF1 and LF2) for the different projections at 40 cm and 70 cm is given in Table 7. The lead-free aprons show no noticeable difference compared to lead aprons, irrespective of the simulation conditions. For the three aprons, the larger the distance the lower the effectiveness. These slight decreases in effectiveness are mostly due to decreased effectiveness for some organs like lungs, oesophagus, brain and heart (Table 8). The dose reduction obtained for the dosimeter placed below the apron on the phantom torso is close to the effective dose reduction. The mean relative difference is 3.5 % for the lead apron and 6 % for the lead-free aprons. However, in some cases, this difference changes drastically. For instance, for LLAT at 70 cm, the

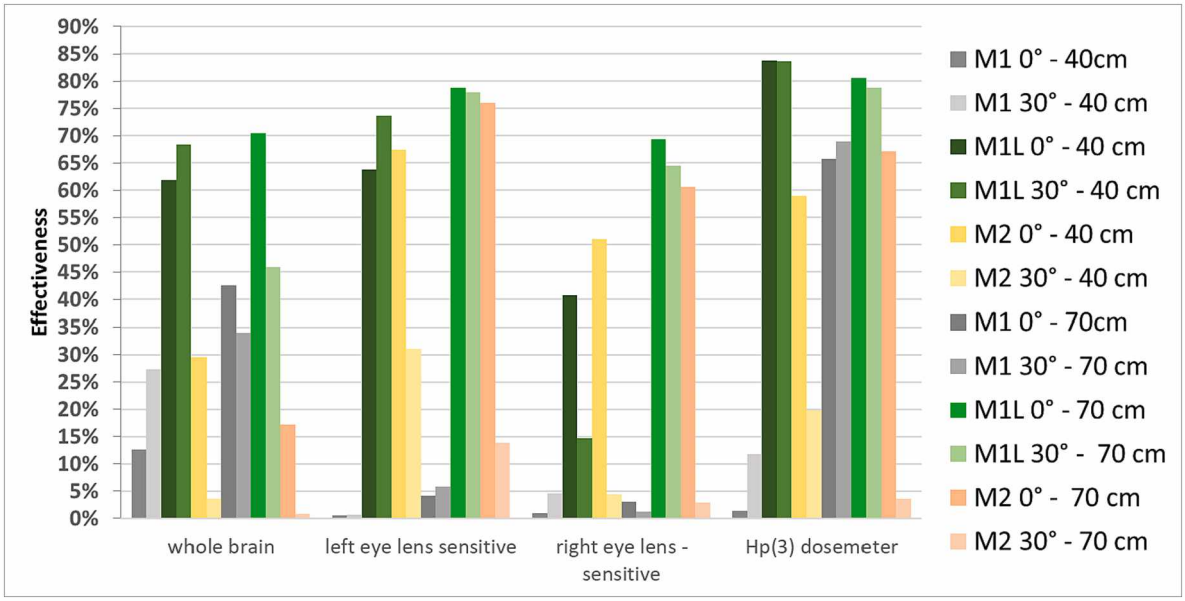

Fig. 8. Simulated dose reduction effectiveness for M1, M1L and M2 at the level of the brain, eye lens and $H_p(3)$ dosimeter, considering two operator head positions (0 and 30°) and distances (40 and 70 cm).

Table 6
Simulated dose reduction effectiveness obtained for the lead and lead-free caps averaged over the five projections at 40 cm and 70 cm.

–	Whole brain (head 0°)		Whole brain (head 30°)		Left eye lens (head 0°)		$H_p(3)$ dosemeter (head 0°)	
	Lead cap	Lead-free cap	Lead cap	Lead-free cap	Lead cap	Lead-free cap	Lead cap	Lead-free cap
70 cm	37 %	39 %	55 %	51 %	1 %	0.6 %	1.6 %	0.8 %
40 cm	14 %	13 %	30 %	28 %	0.4 %	0.3 %	0.9 %	0.3 %

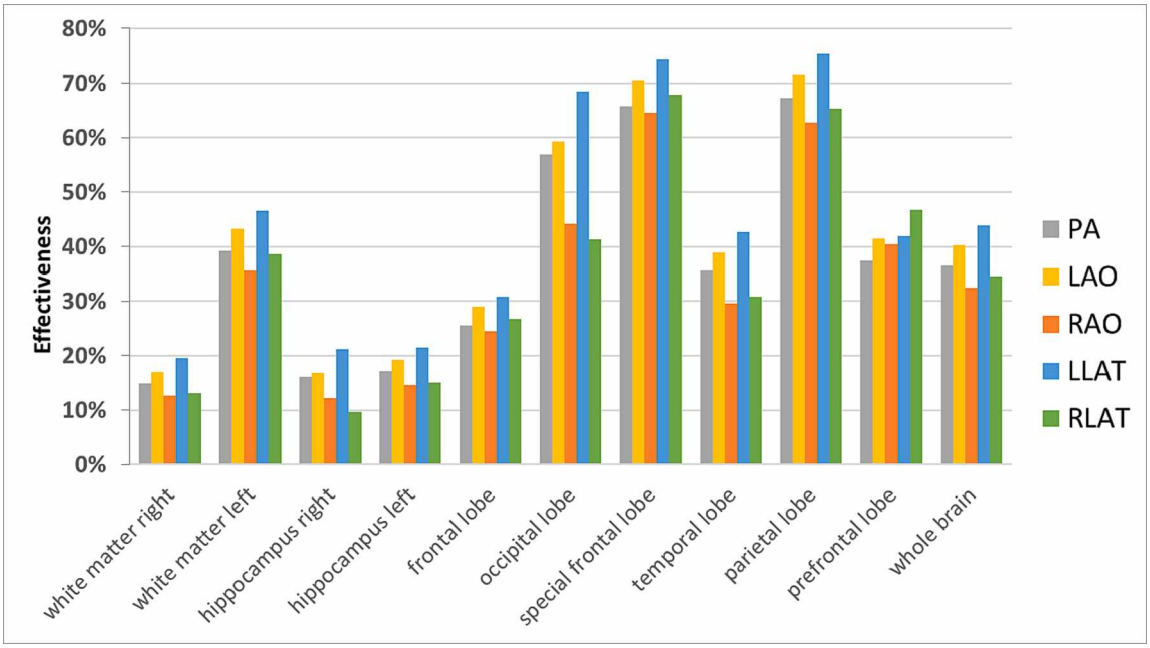

Fig. 9. Simulated dose reduction effectiveness for the different parts of the brain obtained for the lead cap at 70 cm (head at 0°).

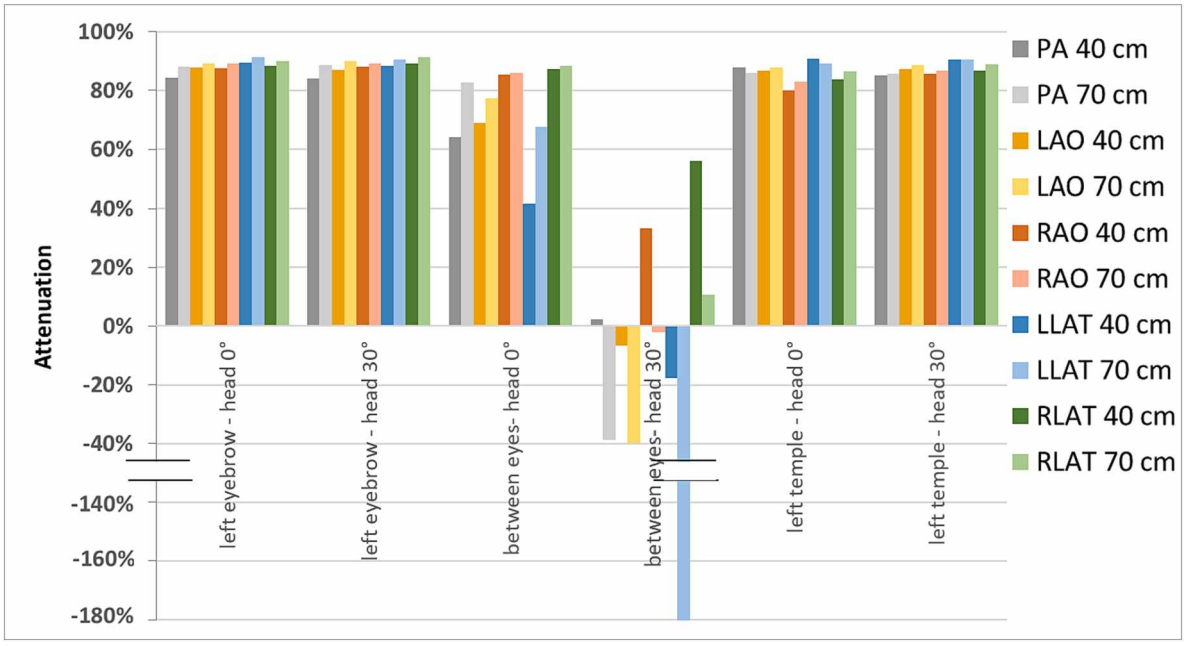

Fig. 10. Lead cap attenuation obtained from the dosimeters placed above and below the cap, at 40 cm and 70 cm and for the head at 0° and 30°.

dose reduction obtained for the dosimeter is around 33 % for the three aprons whereas it is around 79 % for the effective dose.

Patient drapes

In a fixed clinical setting, the dose reduction effectiveness for the head region, resulting from MC calculations and phantom

Table 7
Simulated dose reduction effectiveness obtained for the lead and lead-free aprons for the different projections at 40 cm and 70 cm.

		Lead apron		Lead-free apron 1		Lead-free apron 2	
		Effective dose	Dosimeters	Effective dose	Dosimeters	Effective dose	Dosimeters
70 cm	PA	82%	86%	79%	84%	80%	87%
	LAO45	83%	81%	80%	79%	81%	79%
	RAO45	84%	91%	80%	90%	82%	90%
	LLAT	81%	34%	77%	30%	78%	33%
	RLAT	75%	93%	71%	91%	73%	92%
40 cm	PA	93%	93%	90%	91%	91%	91%
	LAO45	93%	93%	91%	92%	92%	92%
	RAO45	96%	98%	92%	97%	94%	98%
	LLAT	92%	85%	90%	80%	92%	92%
	RLAT	86%	96%	82%	95%	84%	96%

Table 8
Comparison of the lead apron simulated dose reduction effectiveness between 40 cm and 70 cm for some organs of interest.

	Effectiveness 70 cm	Effectiveness 40 cm	Effectiveness 40 cm / Effectiveness 70 cm
Colon	97 %	98 %	1.0
Lungs	**47 %**	**75 %**	**1.6**
Stomach	92 %	95 %	1.0
Breast	96 %	97 %	1.0
Gonads	99 %	100 %	1.0
Bladder	99 %	99 %	1.0
Œsophagus	**63 %**	**83 %**	**1.3**
Liver	93 %	97 %	1.0
Brain	**4 %**	**30 %**	**7.4**
Salivary glands	**19 %**	**49 %**	**2.5**
Intestine	97 %	98 %	1.0
Heart	**72 %**	**89 %**	**1.2**
Kidneys	95 %	96 %	1.0
Prostate	99 %	99 %	1.0
Spleen	81 %	88 %	1.1

measurements, was low. Different projections resulted in simulated effectiveness around 3 % on average for the brain and the eye lens whereas measured effectiveness was below 7 % on average for the eye lenses and not meaningful at the level of the brain. The simulated effectiveness was slightly higher at 70 cm (2.9 %, 3.8 % and 4.4 % for the brain, the left and the right eye, respectively) compared to 40 cm (1.6 %, 2.3 % and 2.5 % for the brain, the left and the right eye, respectively). The drape was more efficient for RAO45 projections for both operator positions: for that projection, the effectiveness ranged from 5.9 % to 10.5 %. No statistical difference was observed between effectiveness for the eye lens ($H_p(3)$) dosimeters and for the actual eye lens. Specific brain regions show dose reduction trends, according to the combination of operator distances and projections, which are comparable to the trends observed for the complete brain.

Significant dose reduction was observed for organs situated in the direct vicinity of the drape, such as the hand skin and, to a lesser extent, the forearm skin (Table 9). In particular, an effectiveness of 62 % and 30 % is observed to the left and right hands, respectively, when they are directly situated above the drape (40 cm). A decrease up to 72 % and 40 % is observed for the left hand in RAO45 and for the right hand in RLAT, respectively. In contrast, effectiveness for the left and right hands is only 18 % and 8 % when the hands are further away from the drape (70 cm). Reduction to other extremities, not in the close vicinity of the drape, is much more limited (forearm) or not observed (leg).

The drape also appears to decrease the dose to some organs situated in the abdomen region, although already protected by the apron, but only for right RLAT projections. For instance, an effectiveness of 18 % and 48 % is observed for the uterus in RLAT at 40 cm and 70 cm, respectively. Absolute dose reduction, however, is small since the lead apron offers an important effectiveness as evidenced by the results in Table 8.

Zero Gravity

Results of Monte Carlo simulations for the ZG are presented in Fig. 11 and Table 10. Different projections resulted in average dose reduction of at least 90 % for all the organs in the head and neck region (Fig. 11) while for organs normally covered by the apron (Table 10) the average dose reduction ranged from 23 % to 81 %. Negative dose reduction (dose increase) was observed for the left lung and the stomach.

Discussion

Masks

Mask attenuation assessed by means of MC simulations obtained from dosimeters placed above and below the mask was very high (82 %) and similar whatever the projections. This attenuation is however not representative of the dose reduction (effectiveness) for the organs and tissues located in the head. Indeed, nearly all the radiation which directed to the dosimeters placed below the mask reaches the mask and are thus attenuated. However, the path of radiation reaching the organs located in the head does not necessarily cross the mask. The magnitude of this effect depends on the mask design and length. For instance, M1 dose reduction effectiveness for the eye lens is very low, either by Monte Carlo simulation (less than 8 %) or by phantom measurements (below 10 %). This suggests that most of the radiations reaching the eye when wearing M1 do not pass through the mask but through the gaps between the mask and the face and thus are not attenuated as shown by Koukorava *et al.* [36] for RP glasses. A better protection of the eye lens is obtained with M1L which is a version of M1 extended towards the chin. This is also confirmed, on one hand, by enhanced eye lens effectiveness

Table 9
Simulated dose reduction effectiveness of the drape for the arm skin and the hand skin at 40 cm and 70 cm.

	40 cm						70 cm					
	PA	LAO45	RAO45	LLAT	RLAT	Mean	PA	LAO45	RAO45	LLAT	RLAT	Mean
Forearm skin (left)	4 %	3 %	10 %	0 %	8 %	**5 %**	18 %	19 %	26 %	3 %	24 %	**18 %**
Forearm skin (right)	19 %	18 %	24 %	3 %	27 %	**18 %**	12 %	16 %	20 %	9 %	13 %	**14 %**
Hand skin (left)	64 %	68 %	72 %	36 %	71 %	**62 %**	21 %	16 %	22 %	9 %	24 %	**18 %**
Hand skin (right)	30 %	30 %	37 %	12 %	40 %	**30 %**	8 %	10 %	9 %	6 %	7 %	**8 %**

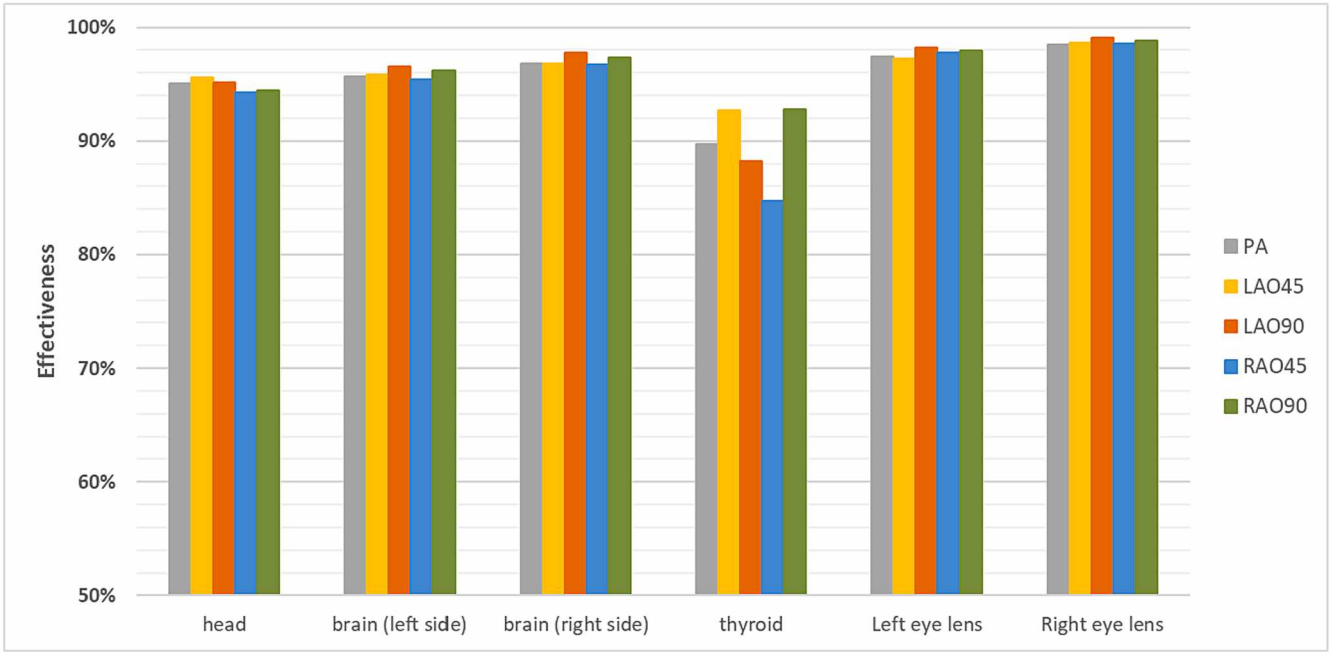

Fig. 11. Simulated dose reduction effectiveness of ZG to various organs in the head region for various projections at 70 cm from the primary beam.

Table 10
Simulated dose reduction effectiveness of ZG system for various projections at 70 cm from the primary beam.

Tissue	PA	LAO45	LLAT	RAO45	RLAT
Left lung	40 %	41 %	46 %	5 %	−18 %
Right lung	79 %	80 %	83 %	73 %	69 %
Stomach	71 %	77 %	76 %	66 %	−18 %
Large intestine	90 %	88 %	88 %	90 %	48 %
Heart	73 %	73 %	75 %	63 %	60 %
Brain (left)	96 %	96 %	97 %	95 %	96 %
Brain (right)	97 %	97 %	98 %	97 %	97 %
Thyroid	90 %	94 %	88 %	85 %	93 %
Testes	65 %	61 %	55 %	81 %	76 %
Left eye lens	97 %	97 %	98 %	98 %	98 %
Right eye lens	98 %	99 %	99 %	99 %	99 %
Effective dose	77 %	77 %	75 %	77 %	82 %

obtained with M2 which is also long, and on the other hand, by the higher eye lens effectiveness obtained with M1 at 70 cm compared to 40 cm. At larger distances, a smaller proportion of radiation comes from underneath the mask. These results are in agreement with those of Koenig *et al.* [37] who measured on phantoms a dose reduction to the eye lens of 70 % for a mask similar to M2 while a non-significant dose reduction of 20 % was obtained for a mask similar to M1. Regarding dose reduction to the brain with the head at 0°, it was found to be better with M1L at the two distances, followed by M2 and M1 at 40 cm; the contrary was found at 70 cm. Once again, these differences can be explained by the length and the shape of the masks. Longer masks are more efficient at shorter distances. However, as the distance from the source increases, effectiveness of M2 decreases due to its particular shape on the sides. This is even more noticeable when the head is rotated at 30° where its effectiveness drops down to a few percent.

From MC simulations, also the dose reduction at the $H_p(3)$ dosimeter is not representative of reduction to the eye lens, in particular for the short mask M1 at 70 cm. Relying on effectiveness values determined using $H_p(3)$ dosimeters could thus lead to a severe underestimation of the real eye lens dose. Similar findings are obtained with phantom measurements: $H_p(3)$ effectiveness ranged from 33 % to 50 % while eye lens effectiveness was less than 10 %. The location of $H_p(3)$ dosimeter can explain this difference: it was located on the left temple closer to the mask surface than the left eye. The additional calculations performed with the operator at 50 cm and 60 cm with M1 indicated that the effectiveness at the $H_p(3)$ dosimeter increased between 60 cm and 70 cm. This suggests that between these two distances, the majority of the radiation which reached the dosimeter from underneath the mask came through the mask.

Finally, comparable efficiencies (around 40 %) are obtained with M1 mask for the whole brain both with simulations and phantoms measurements.

Caps

From MC simulations, an average cap attenuation of 86 % was obtained from the dosimeters positioned directly above and below the lead and lead-free caps. This is in agreement with the 85 % obtained by Uthoff *et al.* [15] from measurements on staff and with the attenuation of 81 % and 86 % obtained from phantom measurements at the left eyebrow and left temple respectively [33]. The attenuation level, however, could be lower (around 50 % on average) in clinical conditions from dosimeters worn above and below a lead-free cap by medical staff [33]. The cap effectiveness obtained from the dosimeters located on the middle of the forehead was less than the one obtained from the two other locations (left eyebrow and left temple). For the middle of the forehead, the effectiveness obtained for LLAT projection by simulations with the head rotated at 30° was below 0. That means that the dose received by the dosimeter below the cap exceeded the one received by the dosimeter above the cap. A similar behaviour was noticed by Grabowicz *et al.* [33]. This suggests that the radiation reaching the dosimeter may come from underneath the cap or may pass through the dosimeter located inside the cap before passing through the dosimeter outside. For the first hypothesis, it could be due to the fact that the cap does not fit perfectly the head of the numerical phantoms while for the second one it suggests that radiations come from the left side or the back of the head.

In our simulation study, lead and lead-free caps have a potential for significant dose reduction to the brain (up to more than 35 %). However, this strongly depends on the relative position of the physician with respect to the primary X-ray field: with the configuration with the head at 0° the average reduction was only about 13 % at 40 cm whereas it was 37 % at 70 cm. This is in agreement with Silva *et al.* [14] who calculated

an average dose reduction to the brain between 6 % and 15 % at 40 cm. This is also the same magnitude as the 7 % effectiveness obtained by means of phantom measurements with TLD [33] and the 3.3 % effectiveness obtained by Fetterly *et al.* [38] thanks to measurements with radiochromic films in an anthropomorphic phantom. In addition, our MC study revealed that the larger the distance, the better the effectiveness. As suggested with the mask, a smaller proportion of radiations may come from underneath the cap at larger distances.

The MC simulations also showed that attenuation calculated from dosimeters located directly above and below the caps is a poor estimator of the brain protection. Indeed the attenuation derived from the dosimeters (more than 80 % on average) severely overestimated the dose reduction in most configurations (on average between 13 % and 37 % at 40 cm and 70 cm, respectively with the head at 0°). This is in agreement with Silva *et al.* [14] who reported that no dosimeters placed under a cap was appropriate to estimate the brain dose reduction because, on average, only 5 % of the brain exposure penetrated the head through the forehead when the physician was at 40 cm from the X-ray field.

Aprons

Comparable attenuations were obtained for lead and lead-free aprons by means of numerical simulations. This is not in agreement with the study of Schlattl *et al.* [39] who, from MC calculations of air kerma below an apron in a broad primary beam, reported that the shielding capability of lead-free materials composed of Sn and Sn/Bi is much lower than that of lead. This was attributed to the high proportion of low-energy photons created by fluorescence in tin. However, as several parameters are different between our study and the one of Schlattl *et al.* [39] (primary beam versus scattered beam, Sn/Bi versus Sb/Bi, kV and filtration, etc.), comparison of the findings is not straightforward. Effective dose reductions obtained from our MC simulations were also quite similar for lead and lead-free aprons. The reduction was around 3 % less with the lead-free aprons. Schlattl *et al.* [39] reported around 3 % effective dose increase with tin/bismuth shielding at 75 kV compared to lead shielding. This moderate increase, compared to the one observed for air kerma by the same authors, was attributed to the fact that low-energy photons created by fluorescence cannot penetrate deeply into the body. Therefore, they observed a distinctive dose increase only in organs located very superficially, as glandular breast tissue for instance.

The decrease of effectiveness when the distance from the source increases, noticed with numerical simulations, may be attributed to two factors. On one hand, moving away from the source, the shadow created by the apron on the head and neck region could be reduced. This would explain the lower effectiveness obtained for the brain and the thyroid at 70 cm. On the other hand, there are some holes in the apron for the arms. They are not wide but their height can reach 20 cm; thus when the distance from the source increases, the trunk and organs like the heart are more exposed because of the apron holes. It should also be kept in mind that the absolute organ dose usually decreases further away from the primary X-ray field. For instance, the dose to the organs included in the effective dose calculations decreases on average by about 60 % at 70 cm with respect to 40 cm.

Except for LLAT at 70 cm, there was a good agreement between the reduction for the dosimeters and the effective dose. Therefore, the dose reduction to the dosimeters is a good approximation of the apron effectiveness for the effective dose.

Patient drapes

From simulations, a lead-free or lead drape positioned on the patient appeared to be an efficient solution to reduce the dose to the left hand and, possibly, to the right hand. The dose reduction to locations such as the brain, the eye and the WB dosimeter, however, was very low or inexistent. Phantom measurements confirmed these results (from the present study and from [34]). However, considerable variation in the drape effectiveness at the level of the eye lens and the WB dosimeter was observed in clinical studies in IC. From measurements on staff, Musallam *et al.* [40] and Dabin *et al.* [41] reported, average reduction of about 50 % to the left eye and the WB dosimeter (WB not measured in [41]); while Politi *et al.* [42] only found 14 % and 24 % reduction, respectively. In a large clinical trial performed in the frame of the MEDIRAD project [11], 50 % and 53 % decrease in left eye dose and WB dose was measured on average, respectively. The considerable difference in dose reduction effectiveness between the clinical measurements and the MC simulations has to be investigated further.

Zero Gravity

As demonstrated by MC simulations the ZG is equivalent to the lead and lead-free aprons for the organs and dosimeters usually covered by the latter. Similar results were obtained from phantom and staff measurements [13]. In addition, as observed with radiation protection cabin [43], MC simulations showed an important effectiveness for the sensitive organs in the head region. In contrast with the mask and the cap which partially cover the head, the ZG effectiveness was rather homogenous for all tissue and organs in the brain region. Reduction to the eye lens dose ranged from 83 % to more than 95 % depending on the projection. This is in agreement with the study of Savage *et al.* [44] who reported 94 % reduction during various types of interventional procedures and more effective than the 50 % dose decrease to the eye lens reported by Haussen *et al.* [45] during interventional neuroprocedures. The MC simulated results are also consistent with the validation measurements performed on an anthropomorphic phantom showing dose reduction to the brain and eye lens from 66 % up to 96 % [13] and with the phantom measurements performed by Koenig *et al.* [37] who reported a dose reduction to the eye lens of 70 %.

In addition, the MC simulations showed that the ZG system reduced the dose to organs normally protected by the apron by 5 % to 98 %, probably because the apron of the ZG system has a higher lead thickness than a conventional apron. These additional reductions lead to decrease in effective dose of around 80 % for the different projections. One should keep in mind, however, that the absolute dose to those organs is usually low when a lead apron is used and can be 100 times lower than the dose to the unprotected left eye lens for instance.

Surprisingly, simulations also showed a dose increase for some internal organs situated on the left side of the interventional cardiologist body in RLAT projections. For instance, 18 % dose increase was observed at the lung and the stomach. Aside from the low magnitude of the dose to those organs covered by the lead apron as already mentioned, this was probably caused by an inaccurate modelling of the ZG, in particular the tissue providing shoulder and upper arm protection. While in reality this protection can easily fold to provide complete coverage of the upper arm during movements, this is not the case for the model used in the simulations, leaving a fixed air gap between the arm and the protection.

Recommendations

Formulating recommendations is not straightforward since the effectiveness of most devices strongly depends on their design and the exposure conditions. For those personal devices that are directly aimed at protecting the head region, such as the masks, an extended face coverage and the smallest possible gap between the face and the device are crucial parameters to ensure adequate protection. Few devices, such as the ZG suspended system, can offer significant dose reduction in most circumstances. From a practical point of view, other factors, such as ergonomics, ease of use and ease of asepsis should also be taken into consideration when choosing a RP device. The results of the present study were used for producing device-specific recommendation in the form of pros and cons [46].

Limitations of the study

Only the dose reduction effectiveness was investigated in this study. In addition to the effectiveness, the absolute dose should be considered when evaluating the performances of a RP device: low dose reduction effectiveness for a specific tissue which is exposed to a very low dose is not of concern for radiation protection, while low dose reduction to a highly exposed tissue is of concern.

Besides, not all combinations of factors that can adversely affect the effectiveness of the RP devices were investigated. Although various configurations were simulated using MC calculations and phantom measurements, only a limited number of RP device models and designs were tested; and only one X-ray beam quality and a limited number of geometry set-ups were considered for the simulations. A comparison of the effectiveness of mask and glasses to protect the eye lens would also be of interest but is out of scope of the present study. Moreover, the X-ray beam quality used in MC simulations and phantom measurements slightly differ in high voltage (80 kV vs 90 kV, respectively) which had an additional input to observed differences in the effectiveness of RP devices obtained with the use of both methods. Some elements (walls and C-arm for instance) were also not modelled in MC simulations as their contribution to scatter radiation is considered to be negligible. Therefore, the effectiveness of the protective devices deserves to be further investigated for other procedure types with different access routes, staff's orientations and anatomies.

The lead equivalence of the RP device should not be overlooked either. The attenuation characteristics as stated on the equipment label are usually indicative of the lead equivalence of the material (or the resulting X-ray attenuation) in a direct X-ray beam with a specific energy spectrum but they are not likely representative of the dose reduction to any specific organ in clinical conditions [47]. This is of even greater concern for lead-free and light lead material because the material properties cannot be easily extrapolated to other exposure conditions without information on the material composition, which is usually not known by the user. Not all simulations could be performed with the elemental composition since this was not always communicated by the manufacturers. In such cases, the lead equivalence was used; however, it can be considerably lower than the one stated on the device label [48].

Finally, the effectiveness of the RP devices was simulated when used individually. However, this is seldom the case in practice. MC simulations could lead to a better understanding of the combined effects and explain discrepancies found in various studies between simulations and clinical measurements.

Conclusion

The dose reduction effectiveness of five RP devices to reduce staff dose were assessed using MC simulations. Phantom measurements were also performed for masks and drapes to complete the data available in the literature. Lead and lead-free caps and masks have a potential for protecting – some parts of - the brain, while masks could protect the eye lens as well. However, their effectiveness strongly depends on the exposure conditions and the device design, potentially leaving staff unprotected without realising it. Lead-free aprons can offer comparable protection to a lead apron and the ZG system offers a considerable dose reduction to all organs covered. Whatever the RP device, it is advisable to always (re)evaluate the effectiveness in the planned conditions of use.

Funding

The Medirad project has received funding from the Euratom research and training programme 2014–2018 under grant agreement No 755523.

Declaration of Competing Interest

The authors declare that they have no known competing financial interests or personal relationships that could have appeared to influence the work reported in this paper.

References

[1] Struelens L, Dabin J, Carinou E, Askounis P, Ciraj-Bjelac O, Domienik-Andrzejewska J, et al. Radiation-Induced Lens Opacities among Interventional Cardiologists: Retrospective Assessment of Cumulative Eye Lens Doses. Radiat Res 2018;189(4):399–408.

[2] Ciraj-Bjelac O, Rehani MM, Sim KH, Liew HB, Vano E, Kleiman NJ. Risk for radiation-induced cataract for staff in interventional cardiology: is there reason for concern? Catheter Cardiovasc Interv 2010;76:826–34. https://doi.org/10.1002/ccd.22670.

[3] Vano E, Kleiman NJ, Duran A, Rehani MM, Echeverri D, Cabrera M. Radiation cataract risk in interventional cardiology personnel. Radiat Res 2010;174(4):490–5. https://doi.org/10.1667/RR2207.1.

[4] Velazquez-Kronen R, Borrego D, Gilbert ES, Miller DL, Moysich KB, Freudenheim JL, et al. Cataract risk in US radiologic technologists assisting with fluoroscopically guided interventional procedures: a retrospective cohort study. Occup Environ Med 2019;76(5):317–25. https://doi.org/10.1136/oemed-2018-105360.

[5] Roguin A, Goldstein J, Bar O. Brain tumours among interventional cardiologists: A cause for alarm? Report of four new cases from two cities and a review of the literature. EuroIntervention 2012;7:1081–6. https://doi.org/10.4244/EIJV7I9A172.

[6] Roguin A, Goldstein J, Bar O, Goldstein JA. Brain and neck tumors among physicians performing interventional procedures. Am J Cardiol 2013;111(9):1368–72.

[7] Buchanan GL, Chieffo A, Mehilli J, Mikhail GW, Mauri F, Presbitero P, et al. The occupational effects of interventional cardiology: results from the WIN for Safety survey. EuroIntervention 2012;8(6):658–63. https://doi.org/10.4244/EIJV8I6A103. PMID: 23086783.

[8] Rajaraman P, Doody MM, Yu CL, Preston DL, Miller JS, Sigurdson AJ, et al. Cancer risks in U.S. radiologic technologists working with fluoroscopically guided interventional procedures, 1994-2008. Am J Roentgenol 2016;206:1101–9.

[9] Dabin J, Domienik-Andrzejewska J, Huet C, Mirowski M, Vanhavere F. Report on effectiveness of protective devices for staff in interventional procedures. Deliverable 2.19, MEDIRAD project 2021. Available at : Documents download module (europa.eu).

[10] Marshall, et al. An investigation into the effect of protective devices on the dose to radiosensitive organs in the head and neck. Br J Radiol 1992;65(777):799–802. https://doi.org/10.1259/0007-1285-65-777- 799. PMID: 1393418.

[11] McCutcheon K, Vanhaverbeke M, Pauwels R, Dabin J, Schoonjans W, Bennett J, et al. Efficacy of MAVIG X-Ray Protective Drapes in Reducing Operator Radiation Dose in the Cardiac Catheterization Laboratory: A Randomized Controlled Trial. Circ Cardiovasc Interv 2020;13(11):e009627. https://doi.org/10.1161/CIRCINTERVENTIONS.120.009627.

[12] McCutcheon K, Vanhaverbeke M, Dabin J, Pauwels R, Schoonjans W, Desmet W, et al. Efficacy of MAVIG X-Ray Protective Drapes in Reducing CTO Operator Radiation. J Interv Cardiol 2021;2021:1–4. https://doi.org/10.1155/2021/3146104.

[13] Zanca F, Dabin J, Collard C, Alexandre N, De Groote A, Salembier JP, et al. Evaluation of a suspended radiation protection system to reduce operator exposure in cardiology interventional procedures. Catheter Cardiovasc Interv 2021;98(5). https://doi.org/10.1002/ccd.29894.

[14] Silva E, Vanhavere F, Struelens L, Covens P, Buls N. Effect of protective devices in the radiation dose received by the brain of interventional cardiologists. EuroIntervention 2018;13(15):e1778–84. https://doi.org/10.4244/EIJ-D-17-00759.

[15] Uthoff H, Peña C, West J, Contreras F, Benenati JF, Katzen BT. Evaluation of Novel Disposable, Light-Weight Radiation Protection Devices in an Interventional Radiology Setting: A Randomized Controlled Trial. Am J Roentgenol 2013;200(4):915–20. https://doi.org/10.2214/AJR.12.8830.

[16] Sans Merce M, Korchi AM, Kobzeva L, Damet J, Erceg G, Marcos Gonzalez A, et al. The value of protective head cap and glasses in neurointerventional radiology. J Neurointerv Surg 2016;8(7):736–40. https://doi.org/10.1136/neurintsurg-2015-011703.

[17] Lemesre C, Graf D, Bisch L, Carroz P, Cherbuin N, Damet J, et al. Efficiency of the RADPAD Surgical Cap in Reducing Brain Exposure During Pacemaker and Defibrillator Implantation. JACC Clin Electrophysiol 2021;7(2):161–70. https://doi.org/10.1016/j.jacep.2020.08.007.

[18] Pelowitz DB. MCNPX User's Manual. Version 2.7.0, Los Alamos National Laboratory, LA-CP-11-00438 2011.

[19] Goorley T, James M, Booth T, Brown F, Bull J, Cox LJ, et al. Features of MCNP6. Ann Nucl Energy 2016;87:772–83. https://doi.org/10.1016/j.anucene.2015.02.020.

[20] Koukorava C, Carinou E, Ferrari P, Krim S, Struelens L. Study of the parameters affecting operator doses in interventional radiology using Monte Carlo simulations. Rad Meas 2011;46(11):1216–22.

[21] Snyder WS, Ford MR, Warner GG. Estimates of Absorbed Fraction for Monoenergetic Photon Sources Uniformly Distributed in Various Organs and Heterogeneous Model. Report ORNL-4979. Oak Ridge National Laboratory; 1978.

[22] Kramer R, Zankl M, Williams G, Drexler G. The calculation of dose from external photon exposures using reference human phantoms and Monte-Carlo methods. Part

I. The male (ADAM) and female (EVA) adult mathematical phantoms GSF Bericht S-885 1982.
[23] Behrens R, Dietze G. Dose conversion coefficients for photon exposure of the human eye lens. Phys Med Biol 2011;56(2):415–37.
[24] Zubal IG, Harrell CR, Smith EO, Rattner Z, Gindi G, Hoffer PB. Computerized three-dimensional segmented human anatomy. Med Phys 1994;21(2):299–302. https://doi.org/10.1118/1.597290.
[25] Behrens R, Dietze G, Zankl M. Dose conversion coefficients for electron exposure of the human eye lens. Phys Med Biol 2009;54(13):4069–87. https://doi.org/10.1088/0031-9155/54/13/008.
[26] ICRP. Adult Reference Computational Phantoms. ICRP publication 110. Annals of the ICRP 2009; 39(2): 1-166.
[27] Saldarriaga Vargas C, Struelens L, Vanhavere F. The Challenges in the Estimation of the Effective Dose When Wearing Radioprotective Garments. Radiat Prot Dosimetry 2018;178(1):101–11. https://doi.org/10.1093/rpd/ncx081.
[28] Lombardo PA, Vanhavere F, Lebacq AL, Struelens L, Bogaerts R. Development and Validation of the Realistic Anthropomorphic Flexible (RAF) Phantom. Health Phys 2018;114(5):486–99. https://doi.org/10.1097/HP.0000000000000805.
[29] Lombardo PA et al.. D9.104: Database of phantom of different statures and postures. 2018. Available at https://www.concert-h2020.eu/en/Publications under D9.104.
[30] Alazzoni A, Gordon CL, Syed J, Natarajan MK, Rokoss M, Schwalm J-D, et al. Randomized Controlled Trial of Radiation Protection With a Patient Lead Shield and a Novel, Nonlead Surgical Cap for Operators Performing Coronary Angiography or Intervention. Circ Cardiovasc Interv 2015;8(8):e002384. https://doi.org/10.1161/CIRCINTERVENTIONS.115.002384.
[31] Aral N, Duch MA, Ardanuy M. Material characterization and Monte Carlo simulation of lead and non-lead X-Ray shielding materials. *Radiation Physics and Chemistry* 2020; 174. doi:10.1016/j.radphyschem. 2020. doi:10.1016/j.radphyschem.2020.108892.
[32] ICRP. The 2007 Recommendations of the International Commission on Radiological Protection. ICRP publication 103. Ann ICRP. 2007; 37(2-4):1-332. doi: 10.1016/j.icrp.2007.10.003.
[33] Grabowicz W, Masiarek K, Tomasz Górnik T, Grycewicz T, Brodecki M, Dabin J et al.. The effect of lead free cap on the doses to the head of interventional cardiologists working in haemodynamic room, submitted.
[34] Grabowicz W, Domienik-Andrzejewska J, Masiarek K, Gornik T, Grycewicz T, Brodecki M, et al. Effectiveness of pelvic lead blanket to reduce the doses to eye lens and hands of interventional cardiologists and assistant nurses. J Radiol Prot 2017;37:715–27. https://doi.org/10.1088/1361-6498/aa7a70.
[35] Alderson SW, Lanzl LH, Rollins M, Spira J. An instrumented phantom system for analog computation of treatment plans. Am J Roentgenol Radium Ther Nucl Med 1962;87:185–95.
[36] Koukorava C, Farah J, Struelens L, Clairand I, Donadille L, Vanhavere F, et al. Efficiency of radiation protection equipment in interventional radiology: a systematic Monte Carlo study of eye lens and whole body doses. J Radiol Prot 2014;34(3):509–28.
[37] Koenig AM, Etzel R, Greger W, Viniol S, Fiebich M, Thomas RP, et al. Protective Efficacy of Different Ocular Radiation Protection Devices: A Phantom Study. Cardiovasc Intervent Radiol 2020;43(1):127–34. https://doi.org/10.1007/s00270-019-02319-1.
[38] Fetterly K, Schueler B, Grams M, Sturchio G, Bell M, Gulati R. Head and Neck Radiation Dose and Radiation Safety for Interventional Physicians. JACC Cardiovasc Interv 2017;10(5):520–58. https://doi.org/10.1016/j.jcin.2016.11.026.
[39] Schlattl H, Zankl M, Eder H, Hoeschen C. Shielding properties of lead-free protective clothing and their impact on radiation doses. Med Phys 2007;34:4270–80. https://doi.org/10.1118/1.2786861.
[40] Musallam A, Volis I, Dadaev S, Abergel E, Soni A, Yalonetsky S, et al. A randomized study comparing the use of a pelvic lead shield during trans-radial interventions: Threefold decrease in radiation to the operator but double exposure to the patient. Catheter Cardiovasc Interv 2015;85(7):1164–70.
[41] Dabin J, Maeremans J, Berus D, Schoonjans W, Tamborino G, Dens J, et al. Dosimetry during Percutaneous Coronary Interventions of Chronic Total Occlusions. Radiat Prot Dosimetry 2018;181(2):120–218. https://doi.org/10.1093/rpd/ncx303.
[42] Politi L, Biondi-Zoccai G, Nocetti L, Costi T, Monopoli D, Rossi R, et al. Reduction of scatter radiation during transradial percutaneous coronary angiography: a randomized trial using a lead-free radiation shield. Catheter Cardiovasc Interv 2012;79(1):97–102. https://doi.org/10.1002/ccd.22947.
[43] Bhar M, Mora S, Kadri O, Zein S, Manai K, Incerti S. Monte Carlo study of patient and medical staff radiation exposures during interventional cardiology. Phys Med 2021;82:200–10. https://doi.org/10.1016/j.ejmp.2021.01.065.
[44] Savage C, Seale Iv T, Shaw C, Angela B, Marichal D, Rees C. Evaluation of a Suspended Personal Radiation Protection System vs. Conventional Apron and Shields in Clinical Interventional Procedures. Open J Radiol 2013;3:143–51. https://doi.org/10.4236/ojrad.2013.33024.
[45] Haussen DC, Van Der Bom IMJ, Nogueira RG. A prospective case control comparison of the ZeroGravity system versus a standard lead apron as radiation protection strategy in neuroendovascular procedures. J NeuroInterv Surg 2016;8:1052–5. https://doi.org/10.1136/neurintsurg-2015-012038.
[46] MEDIRAD recommendation 3.2, 27-33, Available at Recommended 3 (medirad-project.eu).
[47] Eder H, Schlattl H. Shielding effectiveness of X-ray protective garment. Phys Med 2021;82:343–50. https://doi.org/10.1016/j.ejmp.2021.01.081.
[48] Finnerty M, Brennan PC. Protective aprons in imaging departments: manufacturer stated lead equivalence values require validation. Eur Radiol 2005;15(7):1477–84. https://doi.org/10.1007/s00330-004-2571-2.